

## SUPPLEMENTARY MATERIALS

### Accuracy and precision of the pellet LA-ICP-MS method

Pellet LA-ICP-MS method, a relatively new method for bulk trace element analysis, has been applied to the basic schists for the determination of the trace element compositions (B, Sc, V, Cr, Ni, Cu, Zr, Nb and Hf). The accuracy and the precision of the method were tested by analytical curve determined by one glass standard (NIST SRM 612) and three rock standards (JGb1, JB3 and JA3). These standards cover wide range of matrix compositions from basaltic to andesitic. The reference values for the analytical curve were derived from Jochum *et al.* (2011) for all the elements in NIST SRM 612, from Makishima and Nakamura (2006) for Sc, V, Ni, Cu in JB3 and JA3, from Navarro *et al.* (2008) for Zr, Nb, Hf in JGb1 and from Imai *et al.* (1995) for all the other elements in JGb1, JB3 and JA3. Linear relations between the net counts in cps and the reference values in ppm were observed for all the elements (Fig. S1). The analytical values are within  $\pm 10\%$  from the reference concentrations for Cr, Ni, Zr and Hf, and within  $\pm 15\%$  for B, Sc, V, Cu and Nb, except for V in JGb1 (Fig. S2). These agreements with the reference values represent that the accuracy of the analysis is within 10–15% for all the elements. The RSD for the measurement was estimated based on variability of the repeated line-analysis (Fig. S3), and is less than 10% for JB3 except for Cr, less than 17% for JA3 and 20% for JGb1 except for Ni. Although these RSD values are larger than those of the solution ICP-MS method (i.e., ~5%), they are fairly small compared to the variability of the compositions of the samples. The precision and accuracy of the pellet ICP-MS method are precise and accurate enough for the purpose of this study.

### Analytical methods for the determination of major and trace element composition of minerals, and bulk Sr–Nd–Pb isotope composition

Thin sections were made perpendicular to the schistosity and parallel to the lineation. Petrographic observations were conducted by optical microscope as well as electron probe micro analyzer (EPMA). Major element compositions of the constituent minerals were analyzed by EPMA JEOL 8200 equipped in University of Tokyo, and JEOL 8800 in Tokyo Institute of Technology. The accelerating voltage, beam current and beam diameter were 15 kV, 12 nA and 1–5  $\mu\text{m}$ , respectively.

Separation and measurement of Sr–Nd–Pb isotopes were conducted in the Kochi Institute for Core Sample Research, JAMSTEC. The Sr and Nd isotope ratios were determined with a thermal ionization mass spectrometer (TIMS), Thermo TRITON, after chemical separation of Sr and Nd using ion-exchange resin columns. For Sr isotope measurement, faraday collectors were used for si-

multaneous detection of  $^{84}\text{Sr}$ ,  $^{85}\text{Rb}$ ,  $^{86}\text{Sr}$ ,  $^{87}\text{Sr}$  and  $^{88}\text{Sr}$ .  $^{87}\text{Rb}$  interference on  $^{87}\text{Sr}$  was corrected by  $^{87}\text{Rb}/^{85}\text{Rb} = 0.386$ . The effect of mass fractionation was corrected by normalization to  $^{88}\text{Sr}/^{86}\text{Sr} = 8.3752$ . The standard solution NIST SRM 987 was used to calibrate the Sr isotopic ratio. The analysis of NIST SRM 987 and rock standard JB3 gave  $^{87}\text{Sr}/^{86}\text{Sr}$  ratio with mean values  $\pm 2\sigma$  of  $0.7102542 \pm 0.0000042$  and  $0.7034224 \pm 0.0000092$ , respectively. The 2RSDs for samples were lower than 0.0017%. For Nd isotope measurement, faraday collectors were used for counting  $^{142}\text{Nd}$ ,  $^{143}\text{Nd}$ ,  $^{144}\text{Nd}$ ,  $^{145}\text{Nd}$ ,  $^{146}\text{Nd}$  and  $^{147}\text{Sm}$ .  $^{144}\text{Sm}$  interference on  $^{144}\text{Nd}$  was corrected by  $^{144}\text{Sm}/^{147}\text{Sm} = 0.2048$ . The effect of mass fractionation was corrected by normalization to  $^{146}\text{Nd}/^{144}\text{Nd} = 0.7219$ . A Nd isotopic reference material JNDI (Tanaka *et al.*, 2000) was used as the standard, and a repeated analytical  $^{143}\text{Nd}/^{144}\text{Nd}$  value of  $0.5121107 \pm 0.0000064$  ( $2\sigma, n = 3$ ) was obtained. The analysis of rock standard JB3 gave  $^{143}\text{Nd}/^{144}\text{Nd}$  ratio with mean value  $\pm 2\sigma$  of  $0.5130468 \pm 0.0000078$ . The 2RSDs for unknown samples were lower than 0.0022%.

The procedure of Pb separation from rock samples and analysis of Pb isotope by multiple collector ICP-MS (MC-ICP-MS; NEPTUNE, Thermo Fisher Scientific) were followed by Tanimizu and Ishikawa (2006). Faraday collectors were used to count simultaneously  $^{202}\text{Hg}$ ,  $^{203}\text{Tl}$ ,  $^{204}\text{Pb}$ ,  $^{205}\text{Tl}$ ,  $^{206}\text{Pb}$ ,  $^{207}\text{Pb}$  and  $^{208}\text{Pb}$ . The observed  $^{206}\text{Pb}/^{204}\text{Pb}$ ,  $^{207}\text{Pb}/^{204}\text{Pb}$  and  $^{208}\text{Pb}/^{204}\text{Pb}$  ratios were normalized using the  $^{205}\text{Tl}/^{203}\text{Tl}$  ratio of NIST SRM 997, a Tl isotope reference material added to the sample prior to the analysis. In-house standard “cica200” was used to check the absolute value of Pb isotopic ratios and stability of the analysis, which had been crosschecked with NIST SRM 981. The 2RSD of the standard solution for  $^{206}\text{Pb}/^{204}\text{Pb}$ ,  $^{207}\text{Pb}/^{204}\text{Pb}$ , and  $^{208}\text{Pb}/^{204}\text{Pb}$  were 0.010, 0.010 and 0.014%, respectively. The analysis of rock standard JB2 gave mean values  $\pm 2\sigma$  of  $18.3235 \pm 0.0004$ ,  $15.5469 \pm 0.0004$  and  $38.2211 \pm 0.0014$  for  $^{206}\text{Pb}/^{204}\text{Pb}$ ,  $^{207}\text{Pb}/^{204}\text{Pb}$ , and  $^{208}\text{Pb}/^{204}\text{Pb}$ , respectively. 2RSDs for samples were lower than 0.014, 0.014, and 0.016% for  $^{206}\text{Pb}/^{204}\text{Pb}$ ,  $^{207}\text{Pb}/^{204}\text{Pb}$ , and  $^{208}\text{Pb}/^{204}\text{Pb}$ , respectively. For all the isotope ratios, the age correction was calculated by the Rb/Sr, Sm/Nd, Th/Pb and U/Pb ratios obtained by the solution analysis by ICP-MS.

The trace element compositions of minerals were determined with femtosecond LA-ICP-MS equipped in the Tokyo Institute of Technology. A focused laser beam with the approximate energy density of  $15 \text{ J/cm}^2$ , the diameter of  $\sim 20 \mu\text{m}$  and the repetition rate of 10 Hz was used to ablate samples on the spirally moving stage, and as a result, a cylinder-shaped spot with diameter of  $\sim 40 \mu\text{m}$  and depth of  $\sim 40 \mu\text{m}$  was obtained. He gas was used as carrier and the measurement was conducted with Ar gas flow rate of 0.8 l/min and He gas flow rate of 0.6 l/min. Inclu-

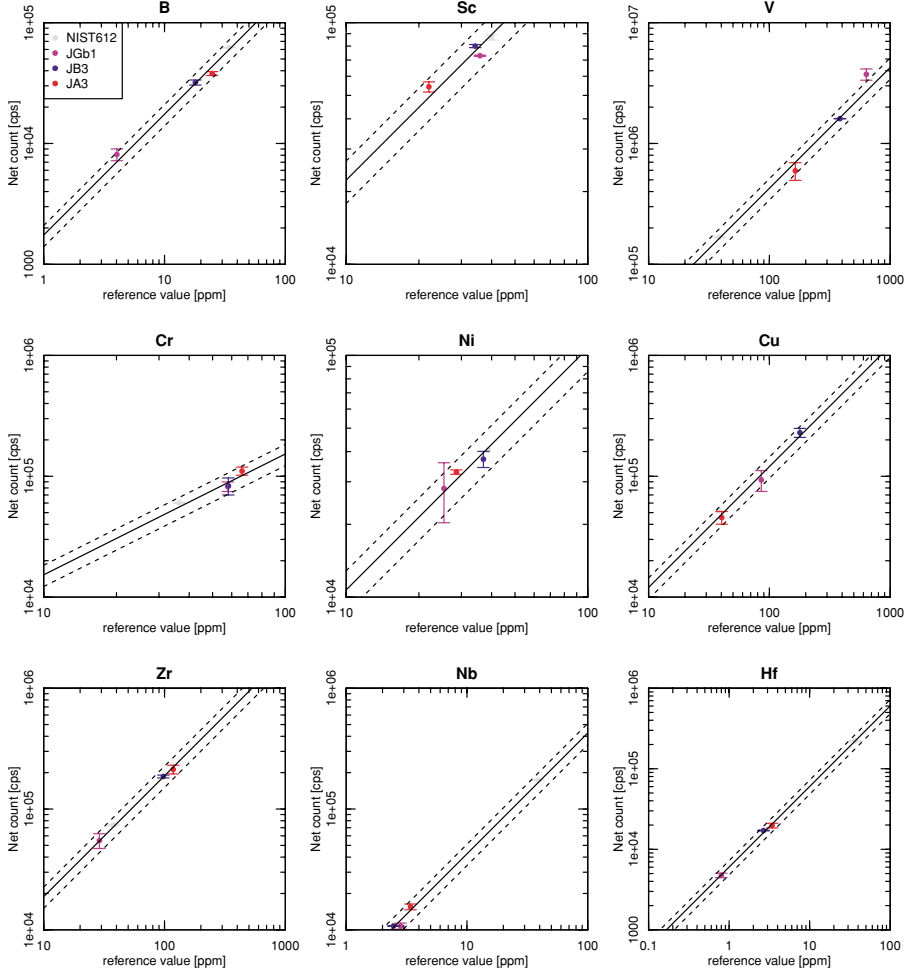


*Fig. S1.* Analytical curves for pellet LA-ICP-MS method. The solid lines indicate the analytical curves ( $y = ax$ ), the dotted lines indicate  $\pm 20\%$  from the analytical curves. The error bars on the plots are RSD of the measurements.

sions in the target minerals have been carefully avoided by *in-situ* microscopic inspection (with transmitted and reflected lights) under the same optical system with the laser beam. The analysis was conducted for 40 seconds: the samples were ablated for the first 10 seconds. The signals were measured for 40 seconds including the peak signals in the first 10 seconds and decaying signals in the following 30 seconds. The background was separately measured for 40 seconds just before each analysis. The glass sample NIST SRM 612 was used as a standard with the recommended concentration (Pearce *et al.*, 1997). The measured  $^{29}\text{Si}$  and  $^{44}\text{Ca}$  intensities were used for internal standard calibration, being compared with the Si and Ca content of the same sample measured by EPMA. The RSD for NIST SRM 612 was 5–15%, depending on the elements ( $n = 15$ ).

#### Garnet-breakdown reaction at the early stage of hydration in the amphibolite body in oligoclase–biotite zone

Garnet-breakdown reaction is indicated from the chlorite exhibiting pseudomorph after garnet. Matrix garnet exists only in the samples with amphibole composition with barroisite  $\rightarrow$  Al-rich hornblende, and not in the samples with ( $\pm$ barroisite  $\rightarrow$ ) Al-rich hornblende  $\rightarrow$  Al-poor hornblende ( $\pm \rightarrow$  actinolite) (Table S1). This correlation of garnet disappearance with amphibole composition indicates the garnet-forming reaction had occurred at the beginning of hydration. Based on the compositions of amphibole and garnet in the garnet–amphibolite, and those of chlorite, amphibole, epidote and plagioclase in the epidote–amphibolite with chlorite pseudomorph after garnet, the mass balance for the garnet-breakdown reactions were solved (Table S2). The compositions of

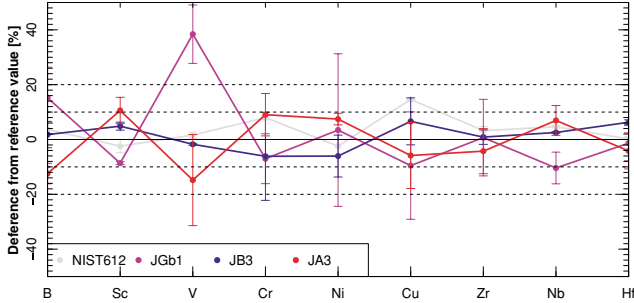


Fig. S2. Difference from the reference values for the concentrations of the standards determined by pellet LA-ICP-MS method. The error bars indicate the RSD of the measurements (see Fig. S3).

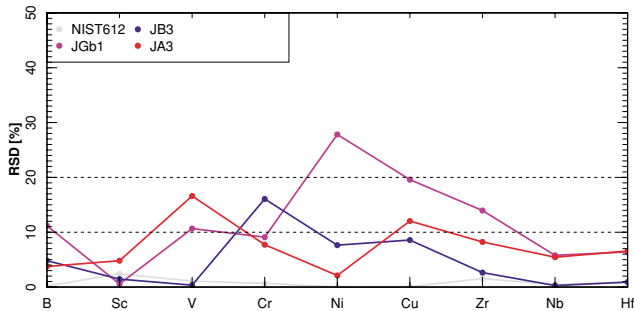
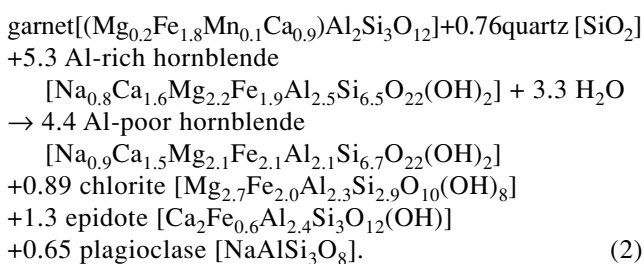


Fig. S3. RSD of the measurement determined by repeated line analysis for pellet LA-ICP-MS method.

the garnet are almandine-rich, typically like  $(\text{Mg}_{0.2}\text{Fe}_{1.8}\text{Mn}_{0.1}\text{Ca}_{0.9})\text{Al}_2\text{Si}_3\text{O}_{12}$ . The compositions of the amphibole in epidote–amphibolite is slightly poorer in Al compared to those in garnet–amphibolite, exhibiting more actinolitic hornblende.  $X_{\text{pst}}$  in epidote ranges 0.6–0.7. Mg/(Mg+Fe) in chlorite replacing the garnet is around 0.6. The albite content of the plagioclase is around 0.99. Assuming closed system for  $\text{Si}^{4+}$ ,  $\text{Al}^{3+}$ ,  $\text{Fe}^{\text{tot}} (= \text{Fe}^{2+} + \text{Fe}^{3+})$ ,  $\text{Mg}^{2+}$ ,  $\text{Ca}^{2+}$  and  $\text{Na}^+$ , the mass balance equation was solved (Table S2). As a result, the garnet-breakdown reaction is referred to as follows:



The obtained reaction is consistent with the observation

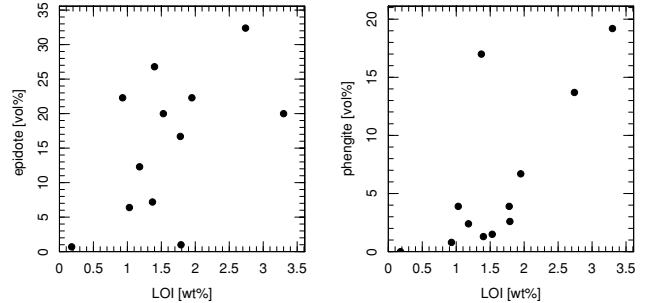


Fig. S4. Relations between mode of epidote and phengite and LOI (loss on ignition). Carbonate-rich samples are excluded from the plots.

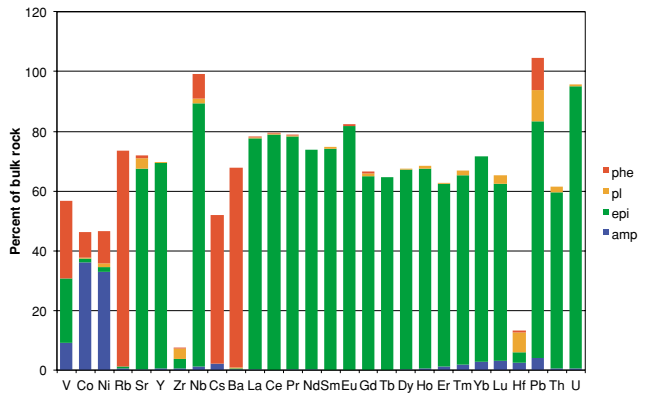


Fig. S5. Trace element distribution in greenschist (ASM019, one of the most hydrated samples). The percentages of elements hosted in each mineral are plotted as vertical axis.

that chlorite occurs as product of garnet hydration (i.e., chlorite pseudomorph after garnet). Al-rich hornblende observed in the garnet–amphibolite is on the reactant side and Al-poor hornblende as well as epidote and plagioclase in the epidote–amphibolite are on the product side, which is also consistent with the occurrence of these minerals.

#### Mobility of HFSE and REE during Sanbagawa metamorphism

Partitioning of HFSE and REE between aqueous fluid and minerals are very low in the  $P-T$  conditions of the Sanbagawa metamorphism (e.g., a peak  $P-T$  condition of 1.0 GPa and 600°C for OBZ); fluid/bulk rock partition coefficients ( $D^{\text{fluid-rock}}$ ) are  $10^{-4}$ – $10^{-6}$  for HFSE and REE whereas 0.1–1000 for Li, Rb, Cs, Ba and Pb, based on the experimental results (Kessel *et al.*, 2005) and their extrapolation to 600°C.  $D^{\text{fluid-rock}}$  of HFSE and REE may increase when the fluid composition becomes rich in  $\text{CO}_2$ , Cl or F. However, fluid inclusion analyses from the

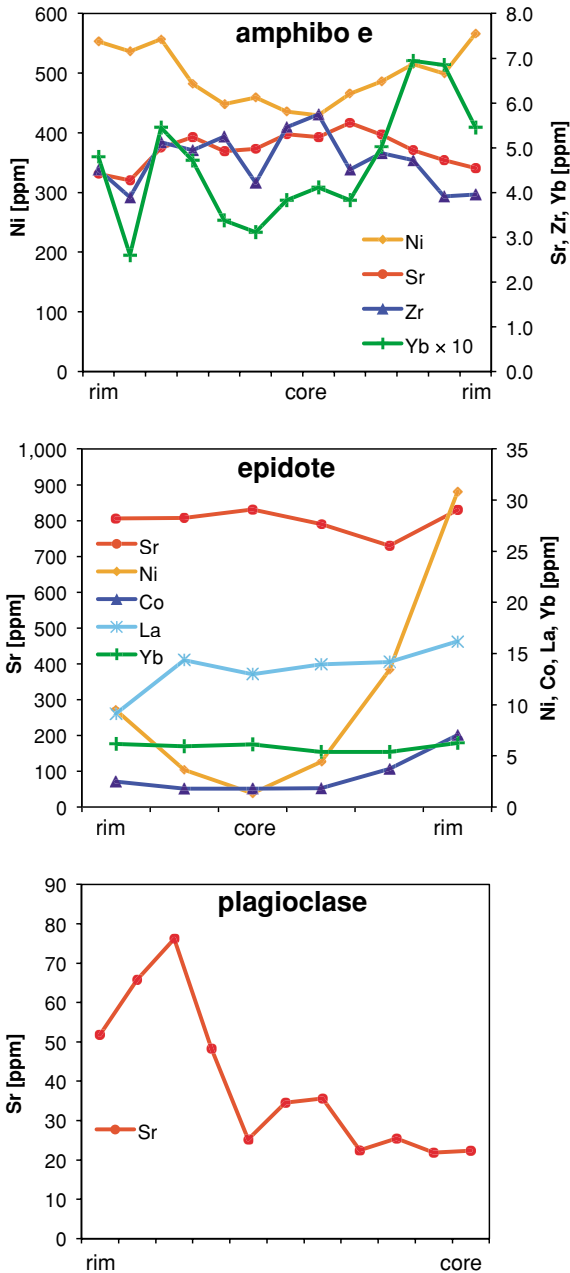


Fig. S6. Compositional zoning of trace elements in amphibole, epidote and plagioclase.

foliation-parallel veins in OBZ indicate that the dominant anion in fluid is  $\text{HCO}_3^-$  (Hirajima *et al.*, 2012). Petrological analyses indicate that  $X_{\text{CO}_2}$  in the OBZ pelitic schists is relatively low (0.06–0.2, based on ; Goto *et al.* (2007); Itaya and Banno (1980)). These lines of evidence indicate that HFSE and REE are relatively immobile during the hydration reaction recorded in the studied basic schists.

#### Partition coefficients used for estimation of fluid compositions

The partition coefficients of phengite are derived from the 2 GPa and 600°C experiment for Cs, Rb and K (Melzer and Wunder, 2001) and the constraints from the natural samples for Ba (Zack *et al.*, 2001; Table S4). The temperature dependent partition coefficients for zoisite is well characterized by experiments at 2 GPa, 750–900°C (Feineman *et al.*, 2007), whose extrapolation is consistent with the partition coefficients constrained by natural sample at 0.5–1.5 GPa, 550°C (Brunsmann *et al.*, 2001). According to the analysis of epidote and zoisite coexisting in a zoisite-quartz vein generated at eclogite-facies/amphibolite-facies transition (Chen *et al.*, 2012), epidote/zoisite partition coefficient is 0.4, 0.5 and 4–6 for Sr, Pb and REE, respectively. The extrapolation of the experiment data to 600°C (Feineman *et al.*, 2007) was corrected by epidote/zoisite partition coefficient derived from Chen *et al.* (2012), and was adopted for the mineral/fluid partition coefficient of epidote for REE, Sr and Pb (Table S4).

#### REFERENCES

- Brunsmann, A., Franz, G. and Erzinger, J. (2001) REE mobilization during small-scale high-pressure fluid-rock interaction and zoisite/fluid partitioning of La to Eu. *Geochim. Cosmochim. Acta* **65**, 559–570.
- Chen, R.-X., Zheng, Y.-F. and Hu, Z. (2012) Episodic fluid action during exhumation of deeply subducted continental crust: Geochemical constraints from zoisite-quartz vein and host metabasite in the Dabie orogen. *Lithos* **155**, 146–166.
- Feineman, M. D., Ryerson, F. J., DePaolo, D. J. and Plank, T. (2007) Zoisite-aqueous fluid trace element partitioning with implications for subduction zone fluid composition. *Chem. Geol.* **239**, 250–265.
- Goto, A., Kunugiza, K. and Omori, S. (2007) Evolving fluid composition during prograde metamorphism in subduction zones: A new approach using carbonate-bearing assemblages in the pelitic system. *Gondwana Res.* **11**, 166–179.
- Hirajima, T., Yoshida, K., Sengen, Y., Noguchi, N., Kobayashi, T., Mishima, T. and Ohsawa, S. (2012) Li/B ratio of crush-leached fluid obtained from the Sanbagawa metamorphic belt: Its areal distribution. *Japan Geoscience Union Meeting Abstract SCG65-P11*.
- Imai, N., Terashima, S., Itoh, S. and Ando, A. (1995) Compilation of analytical data for minor and trace elements in seventeen GSJ geochemical reference samples, “igneous rock series”. *Geostand. Newslett.* **19**, 135–213.
- Itaya, T. and Banno, S. (1980) Paragenesis of titanium-bearing accessories in pelitic schists of the Sanbagawa metamorphic belt, central Shikoku, Japan. *Contrib. Mineral. Petrol.* **73**, 267–276.
- Jochum, K. P., Weis, U., Stoll, B., Kuzmin, D., Yang, Q., Raczek, I., Jacob, D. E., Stracke, A., Birbaum, K., Frick, D. A., Günther, D. and Enzweiler, J. (2011) Determination of reference values for NIST SRM 610-617 glasses following ISO guidelines. *Geostand. Geoanal. Res.* **35**, 397–429.

*Table S1.* Representative compositions of amphibole, garnet, plagioclase, epidote, chlorite and phengite. Units for oxide concentration are in wt%

Amphibole	ASM017			Rim	ASM022			Core	ASM019			Rim	ASM011		
	p1 41	p12 16	p12 20	a2L2-5	a2L2-16	a2L2-24	a2L2-31	a3L1-3	a3L1-12	a3L1-13	a6L1-7	a6L1-9	a6L1-23	a5L1-14	
	SiO <sub>2</sub>	45.53	45.94	45.38	44.08	43.58	46.44	48.85	47.97	48.07	47.40	53.80	50.42	42.49	45.30
TiO <sub>2</sub>	0.48	0.48	0.58	0.41	0.49	0.43	0.26	0.31	0.41	0.22	0.04	0.18	0.69	0.67	
Al <sub>2</sub> O <sub>3</sub>	12.48	12.42	12.24	14.39	15.32	13.31	11.62	10.55	9.75	10.17	2.74	6.16	12.48	12.68	
FeO	16.20	16.61	16.72	14.43	15.34	14.60	14.15	12.64	11.83	11.62	16.49	17.31	18.44	19.06	
MnO	0.17	0.19	0.19	0.12	0.08	0.16	0.06	0.34	0.24	0.21	0.15	0.18	0.38	0.39	
MgO	9.77	9.99	9.66	9.97	9.20	10.65	11.41	12.39	13.47	13.81	13.72	11.62	8.84	8.95	
CaO	9.63	9.57	9.75	10.42	9.63	8.71	8.15	8.52	9.49	9.67	9.74	9.54	9.51	8.31	
Na <sub>2</sub> O	3.00	3.02	3.11	2.47	2.74	3.02	2.98	2.79	2.76	2.50	1.87	2.51	3.14	3.36	
K <sub>2</sub> O	0.37	0.38	0.40	0.35	0.42	0.32	0.20	0.56	0.34	0.34	0.12	0.27	0.84	0.77	
Total	97.66	98.61	98.05	96.69	96.85	97.64	97.82	96.12	96.38	96.00	98.67	98.23	96.80	99.47	
Cations per 23 oxygens															
Si <sup>4+</sup>	6.70	6.70	6.68	6.52	6.44	6.72	6.99	7.00	6.99	6.91	7.72	7.36	6.44	6.60	
Ti <sup>4+</sup>	0.05	0.05	0.06	0.05	0.05	0.05	0.03	0.03	0.04	0.02	0.00	0.02	0.08	0.07	
Al <sup>3+iv</sup>	1.30	1.30	1.32	1.48	1.56	1.28	1.01	1.00	1.01	1.09	0.28	0.64	1.56	1.40	
Al <sup>3+vi</sup>	0.87	0.83	0.81	1.02	1.10	0.99	0.96	0.81	0.67	0.66	0.18	0.41	0.67	0.78	
Fe <sup>3+</sup>	0.20	0.26	0.19	0.17	0.27	0.35	0.39	0.30	0.25	0.34	0.33	0.26	0.29	0.43	
Fe <sup>2+ [M13+M2]</sup>	1.76	1.73	1.85	1.59	1.59	1.38	1.26	1.21	1.17	1.05	1.61	1.82	2.00	1.83	
Fe <sup>2+ [M4]</sup>	0.03	0.03	0.02	0.02	0.03	0.04	0.04	0.03	0.02	0.03	0.03	0.03	0.04	0.06	
Mn <sup>2+</sup>	0.02	0.02	0.02	0.02	0.01	0.02	0.01	0.04	0.03	0.03	0.02	0.02	0.05	0.05	
Mg <sup>2+ [M13+M2]</sup>	2.11	2.13	2.09	2.17	1.98	2.24	2.36	2.64	2.87	2.93	2.87	2.48	1.96	1.88	
Mg <sup>2+ [M4]</sup>	0.03	0.04	0.03	0.03	0.04	0.06	0.07	0.06	0.05	0.07	0.06	0.04	0.04	0.06	
Ca <sup>2+</sup>	1.52	1.49	1.54	1.65	1.52	1.35	1.25	1.33	1.48	1.51	1.50	1.49	1.54	1.30	
Na <sup>+</sup>	0.86	0.85	0.89	0.71	0.79	0.85	0.83	0.79	0.78	0.71	0.52	0.71	0.92	0.95	
K <sup>+</sup>	0.07	0.07	0.07	0.07	0.08	0.06	0.04	0.10	0.06	0.06	0.02	0.05	0.16	0.14	
Total	15.52	15.52	15.58	15.49	15.47	15.38	15.23	15.35	15.42	15.40	15.15	15.35	15.76	15.56	
X <sub>v,A</sub>	0.48	0.48	0.42	0.51	0.53	0.62	0.77	0.65	0.58	0.60	0.87	0.68	0.29	0.48	
X <sub>Na,A</sub>	0.45	0.45	0.50	0.42	0.40	0.32	0.20	0.25	0.36	0.34	0.11	0.27	0.55	0.37	
X <sub>KA</sub>	0.07	0.07	0.07	0.07	0.08	0.06	0.04	0.10	0.06	0.06	0.02	0.05	0.16	0.14	
X <sub>Na,M4</sub>	0.20	0.20	0.19	0.14	0.19	0.26	0.32	0.27	0.21	0.18	0.20	0.22	0.19	0.29	
X <sub>Ca,M4</sub>	0.76	0.75	0.77	0.82	0.76	0.68	0.62	0.67	0.74	0.76	0.75	0.75	0.77	0.65	
X <sub>Mg,M4</sub>	0.02	0.02	0.01	0.01	0.02	0.03	0.04	0.03	0.03	0.04	0.03	0.02	0.02	0.03	
X <sub>Fe,M4</sub>	0.01	0.02	0.01	0.01	0.02	0.02	0.02	0.01	0.01	0.01	0.02	0.02	0.02	0.03	
X <sub>Mn,M4</sub>	0.01	0.01	0.01	0.01	0.01	0.01	0.00	0.02	0.01	0.01	0.01	0.01	0.02	0.02	
X <sub>Mg,M13</sub>	0.54	0.55	0.53	0.58	0.55	0.62	0.65	0.69	0.71	0.74	0.64	0.58	0.49	0.51	
X <sub>Fe,M13</sub>	0.46	0.45	0.47	0.42	0.45	0.38	0.35	0.31	0.29	0.26	0.36	0.42	0.51	0.49	
X <sub>Mg,M2</sub>	0.24	0.24	0.25	0.22	0.16	0.19	0.20	0.29	0.37	0.36	0.48	0.38	0.24	0.18	
X <sub>Fe2+,M2</sub>	0.20	0.19	0.22	0.16	0.13	0.12	0.11	0.13	0.15	0.13	0.27	0.28	0.24	0.18	
X <sub>Fe3+,M2</sub>	0.10	0.13	0.09	0.08	0.13	0.17	0.20	0.15	0.12	0.17	0.17	0.13	0.15	0.22	
X <sub>Al,M2</sub>	0.43	0.41	0.40	0.51	0.55	0.49	0.48	0.41	0.33	0.33	0.09	0.21	0.34	0.39	
X <sub>Ti,M2</sub>	0.03	0.03	0.03	0.02	0.03	0.02	0.01	0.02	0.02	0.01	0.00	0.01	0.04	0.04	
X <sub>Al,T</sub>	0.32	0.33	0.33	0.37	0.39	0.32	0.25	0.25	0.25	0.27	0.07	0.16	0.39	0.35	
X <sub>Si,T</sub>	0.68	0.67	0.67	0.63	0.61	0.68	0.75	0.75	0.75	0.73	0.93	0.84	0.61	0.65	

- Kessel, R., Schmidt, M. W., Ulmer, P. and Pettke, T. (2005) Trace element signature of subduction-zone fluids, melts and supercritical liquids at 120–180 km depth. *Nature* **437**, 724–727.
- Makishima, A. and Nakamura, E. (2006) Determination of major/minor and trace elements in silicate samples by ICP-QMS and ICP-SFMS applying isotope dilution-internal standardisation (ID-IS) and multi-stage internal standardisation. *Geostand. Geoanal. Res.* **30**, 245–271.
- Melzer, S. and Wunder, B. (2001) K–Rb–Cs partitioning between phlogopite and fluid: experiments and consequences for the LILE signatures of island arc basalts. *Lithos* **59**, 69–

- 90.
- Navarro, M. S., Andrade, S., Ulbrich, H., Gomes, C. B. and Girardi, V. A. V. (2008) The direct determination of rare earth elements in basaltic and related rocks using ICP-MS: Testing the efficiency of microwave oven sample decomposition procedures. *Geostand. Geoanal. Res.* **32**, 167–180.
- Pearce, N. J. G., Perkins, W. T., Westgate, J. A., Gorton, M. P., Jackson, S. E., Neal, C. R. and Chereny, S. P. (1997) A Compilation of new and published major and trace element data for NIST SRM 610 and NIST SRM 612 glass reference materials. *Geostand. Geoanal. Res.* **21**, 115–144.
- Tanaka, T., Togashi, S., Kamioka, H., Amakawa, H., Kagami,

Table S1. (continued)

Garnet	Plagioclase				Epidote				Chlorite				Phengite				
	Rim	ASM022		Core	ASM017		ASM017		ASM017		ASM017		ASM017		ASM017		
	g50-1	g50-14	g50-29	g50-41	pl1 26	pl2 11	pl1 33	pl2 6	chl 5	chl 7	ms1-1	ms2-2					
SiO <sub>2</sub>	38.51	37.45	37.46	37.92	SiO <sub>2</sub>	71.43	70.53	SiO <sub>2</sub>	39.44	39.99	SiO <sub>2</sub>	27.80	27.52	SiO <sub>2</sub>	51.34	53.04	
TiO <sub>2</sub>	0.13	0.17	0.18	0.36	TiO <sub>2</sub>	0.06	0.00	TiO <sub>2</sub>	0.09	0.18	TiO <sub>2</sub>	0.00	0.01	TiO <sub>2</sub>	0.67	0.30	
Al <sub>2</sub> O <sub>3</sub>	20.97	20.85	20.69	20.59	Al <sub>2</sub> O <sub>3</sub>	19.51	19.70	Al <sub>2</sub> O <sub>3</sub>	24.89	25.87	Al <sub>2</sub> O <sub>3</sub>	18.87	19.26	Al <sub>2</sub> O <sub>3</sub>	28.21	27.89	
FeO	26.84	27.36	27.85	26.44	FeO	0.12	0.14	FeO	10.01	9.35	FeO	22.44	21.98	FeO	4.78	4.09	
MnO	1.40	2.10	2.70	2.78	MnO	0.03	0.00	MnO	0.02	0.03	MnO	0.36	0.30	MnO	0.14	0.04	
MgO	2.48	1.43	1.52	1.27	MgO	0.00	0.00	MgO	0.02	0.04	MgO	17.04	18.21	MgO	2.66	2.48	
CaO	9.62	10.43	8.77	10.29	CaO	0.30	0.29	CaO	23.03	23.44	CaO	0.13	0.01	CaO	0.01	0.00	
Na <sub>2</sub> O	0.03	0.00	0.01	0.05	Na <sub>2</sub> O	11.01	11.22	Na <sub>2</sub> O	0.00	0.02	Na <sub>2</sub> O	0.01	0.04	Na <sub>2</sub> O	0.59	0.69	
K <sub>2</sub> O	0.00	0.00	0.01	0.00	K <sub>2</sub> O	0.04	0.04	K <sub>2</sub> O	0.02	0.00	K <sub>2</sub> O	0.21	0.01	K <sub>2</sub> O	9.11	9.10	
Total	99.97	99.79	99.19	99.70	Total	102.51	101.91	Total	97.56	98.91	Total	86.86	87.34	Total	97.37	97.67	
Cations per 12 oxygens				Cations per 8 oxygens				Cations per 12.5 oxygens				Cations per 14 oxygens				Cations per 11 oxygens	
Si <sup>4+</sup>	3.04	3.00	3.02	3.03	Si <sup>4+</sup>	3.03	3.01	Si <sup>4+</sup>	3.08	3.07	Si <sup>4+</sup>	2.91	2.86	Si <sup>4+</sup>	3.36	3.44	
Ti <sup>4+</sup>	0.01	0.01	0.01	0.02	Ti <sup>4+</sup>	0.00	0.00	Ti <sup>4+</sup>	0.01	0.01	Ti <sup>4+</sup>	0.00	0.00	Ti <sup>4+</sup>	0.03	0.01	
Al <sup>3+</sup>	1.95	1.97	1.96	1.94	Al <sup>3+</sup>	0.98	0.99	Al <sup>3+</sup>	2.29	2.34	Al <sup>3+</sup>	2.33	2.35	Al <sup>3+</sup>	2.18	2.13	
Fe <sup>2+</sup>	1.77	1.83	1.88	1.77	Fe <sup>2+</sup>	0.00	0.00	Fe <sup>2+</sup>	0.65	0.60	Fe <sup>2+</sup>	1.96	1.91	Fe <sup>2+</sup>	0.26	0.22	
Mn <sup>2+</sup>	0.09	0.14	0.18	0.19	Mn <sup>2+</sup>	0.00	0.00	Mn <sup>2+</sup>	0.00	0.00	Mn <sup>2+</sup>	0.03	0.03	Mn <sup>2+</sup>	0.00	0.00	
Mg <sup>2+</sup>	0.29	0.17	0.18	0.15	Mg <sup>2+</sup>	0.00	0.00	Mg <sup>2+</sup>	0.00	0.00	Mg <sup>2+</sup>	2.66	2.82	Mg <sup>2+</sup>	0.26	0.24	
Ca <sup>2+</sup>	0.81	0.89	0.76	0.88	Ca <sup>2+</sup>	0.01	0.01	Ca <sup>2+</sup>	1.92	1.93	Ca <sup>2+</sup>	0.02	0.00	Ca <sup>2+</sup>	0.00	0.00	
Na <sup>+</sup>	0.00	0.00	0.00	0.01	Na <sup>+</sup>	0.91	0.93	Na <sup>+</sup>	0.00	0.00	Na <sup>+</sup>	0.00	0.01	Na <sup>+</sup>	0.07	0.09	
K <sup>+</sup>	0.00	0.00	0.00	0.00	K <sup>+</sup>	0.00	0.00	K <sup>+</sup>	0.00	0.00	K <sup>+</sup>	0.03	0.00	K <sup>+</sup>	0.76	0.75	
Total	7.98	8.01	7.99	7.98	Total	4.93	4.96	Total	7.95	7.95	Total	9.94	9.97	Total	6.93	6.90	
$X_{prp}$	0.10	0.06	0.06	0.05	$X_{ab}$	0.99	0.99	$X_{czo}$	0.31	0.36	$X_{cln}$	0.35	0.40	$X_{mus}$	0.49	0.52	
$X_{alm}$	0.60	0.60	0.63	0.59	$X_{an}$	0.01	0.01	$X_{pst}$	0.69	0.64	$X_{dph}$	0.40	0.38	$X_{sel}$	0.13	0.12	
$X_{sps}$	0.03	0.05	0.06	0.06				$X_{mnc}$	0.01	0.01	$X_{fec}$	0.13	0.11				
$X_{grs}$	0.27	0.29	0.25	0.30				$X_{ame}$	0.24	0.21	$X_{pyr}$	0.18	0.17				
								$X_{dn}$	0.58	0.60	$X_{pa}$	0.07	0.09				
								$X_{dph}$	0.42	0.40	$X_{mg}$	0.00	0.00				

H., Hamamoto, T., Yuhara, M., Orihashi, Y., Yoneda, S., Shimizu, H., Kunimaru, T., Takahashi, K., Yanagi, T., Nakano, T., Fujimaki, H., Shinjo, R., Asahara, Y., Tanimizu, M. and Dragusanu, C. (2000) JNDI-1: a neodymium isotopic reference in consistency with LaJolla neodymium. *Chem. Geol.* **168**, 279–281.

Tanimizu, M. and Ishikawa, T. (2006) Development of rapid and precise Pb isotope analytical techniques using MC-ICP-MS and new results for GSJ rock reference samples. *Geochim. J.* **40**, 121–133.

Zack, T., Rivers, T. and Foley, S. (2001) Cs–Rb–Ba systematics in phengite and amphibole: an assessment of fluid mobility at 2.0 GPa in eclogites from Trescolmen, Central Alps. *Contrib. Mineral. Petrol.* **140**, 651–669.

Table S2. Representative composition of each mineral used for mass balance calculation (cations per unit formula) and calculated stoichiometric coefficients ( $v_i$ ) for garnet-breakdown reaction

	Reactant in GA				Product in EA			
	grt	amp	qtz	H <sub>2</sub> O	amp	epi	pl	chl
Si <sup>4+</sup>	3.01	6.49	1.00	0.00	6.71	3.07	3.03	2.87
Al <sup>3+</sup>	1.95	2.48	0.00	0.00	2.11	2.32	0.98	2.33
Fe <sup>tot</sup>	1.82	1.86	0.00	0.00	2.07	0.62	0.00	1.99
Mg <sup>2+</sup>	0.19	2.18	0.00	0.00	2.12	0.00	0.00	2.73
Ca <sup>2+</sup>	0.86	1.58	0.00	0.00	1.51	1.93	0.01	0.01
Na <sup>+</sup>	0.00	0.82	0.00	0.00	0.85	0.00	0.91	0.00
H <sup>+</sup>	0.00	2.00	0.00	2.00	2.00	1.00	0.00	8.00
$v_i$	-1	-5.32	-0.76	-3.32	4.42	1.34	0.65	0.89

*Table S3.* Trace element composition of amphibole, epidote, plagioclase and phengite in ASM019, measured by LA-ICP-MS. Units are in ppm

	amphibole													Rim		
	Rim amp-2	amp-3	amp-4	amp-5	amp-6	amp-7	Core amp-8	amp-9	amp-10	amp-11	amp-12	amp-13	amp-14	ave	$1\sigma$	
V	154	151	166	152	145	146	152	143	150	148	152	151	155	151	5.37	
Co	202	198	193	199	194	197	195	195	192	189	198	192	195	195	3.27	
Ni	553	537	557	482	448	459	435	429	465	486	515	499	566	495	45.6	
Rb	3.13	—	3.38	1.56	—	0.97	1.28	—	1.45	1.02	1.89	1.33	—	1.78	0.83	
Sr	4.42	4.27	4.99	5.24	4.93	4.97	5.31	5.24	5.55	5.29	4.95	4.72	4.55	4.96	0.36	
Y	0.86	0.91	1.00	0.94	0.96	1.00	0.94	0.88	0.70	0.75	1.89	0.95	0.93	0.98	0.28	
Zr	4.51	3.89	5.12	4.95	5.25	4.22	5.46	5.74	4.52	4.88	4.73	3.91	3.96	4.70	0.58	
Nb	0.81	—	—	—	—	0.15	0.22	—	—	0.15	0.25	0.17	0.22	0.28	0.22	
Cs	0.29	—	0.32	—	—	—	—	—	—	—	—	—	—	0.31	0.01	
Ba	1.51	0.35	1.93	1.04	0.35	0.36	0.51	0.64	0.69	0.60	1.27	0.71	0.26	0.79	0.49	
La	0.09	0.10	—	0.05	—	0.03	0.12	—	—	0.03	0.05	0.10	0.08	0.07	0.03	
Ce	0.06	—	0.03	—	—	—	0.03	—	0.06	—	0.05	—	—	0.05	0.01	
Pr	—	—	0.03	—	—	0.02	—	—	0.02	—	—	0.02	—	0.02	0.01	
Nd	—	—	—	—	0.10	—	—	—	—	—	—	—	—	0.10	0.00	
Sm	—	—	—	—	—	—	—	—	—	—	—	—	—	—	—	
Eu	—	—	—	—	—	—	—	—	—	—	—	—	—	—	—	
Gd	—	—	—	—	—	—	—	—	—	—	—	—	—	—	—	
Tb	—	—	—	—	—	—	—	—	—	—	—	—	—	—	—	
Dy	0.08	0.14	0.08	0.17	—	0.11	0.14	0.06	0.08	0.05	0.34	0.08	0.11	0.12	0.08	
Ho	0.04	0.03	0.05	0.06	0.03	0.03	0.05	0.05	—	0.03	0.08	—	0.05	0.04	0.02	
Er	0.16	0.22	0.18	0.18	0.14	0.14	0.16	0.20	0.16	0.13	0.38	0.16	0.28	0.19	0.07	
Tm	0.04	0.03	0.05	0.05	0.06	0.06	0.04	0.09	0.02	0.05	0.06	0.05	0.06	0.05	0.02	
Yb	0.48	0.26	0.54	0.47	0.34	0.31	0.38	0.41	0.38	0.50	0.69	0.68	0.55	0.46	0.13	
Lu	0.11	0.06	0.07	0.09	0.08	0.03	0.07	0.08	0.09	0.05	0.14	0.07	0.07	0.08	0.02	
Hf	0.33	0.24	0.33	0.48	0.40	0.23	0.41	0.56	0.17	0.44	0.64	0.45	0.33	0.39	0.13	
Pb	0.19	—	0.13	—	—	0.16	—	—	—	—	—	—	0.13	0.16	0.02	
Th	—	0.02	—	—	—	—	—	—	—	—	—	—	—	0.02	—	
U	—	—	—	—	—	—	—	—	—	—	0.01	—	—	0.01	—	

Table S3. (continued)

	epidote							
	Rim epi-1	epi-2	Core epi-3	epi-4	epi-5	Rim epi-6	ave	$1\sigma$
V	189	179	166	191	201	186	185	10.8
Co	2.48	1.78	1.80	1.83	3.73	7.04	3.11	1.89
Ni	9.48	3.64	—	4.43	13.4	30.8	12.4	9.89
Rb	0.88	—	—	1.12	—	—	1.00	0.12
Sr	806	808	831	791	730	830	799	34.1
Y	53.4	60.3	54.8	52.7	45.2	58.7	54.2	4.88
Zr	2.54	3.19	3.51	2.58	37.9	9.02	9.79	12.8
Nb	—	—	—	3.80	4.46	25.1	11.1	9.88
Cs	—	—	—	—	—	—	—	—
Ba	1.45	0.43	0.41	1.71	0.96	1.59	1.09	0.53
La	9.11	14.4	13.0	13.9	14.2	16.2	13.5	2.17
Ce	26.3	39.1	35.2	40.6	40.8	43.9	37.6	5.69
Pr	4.15	5.48	5.24	5.45	5.12	6.51	5.33	0.69
Nd	18.3	26.7	24.2	28.9	26.0	30.8	25.8	3.96
Sm	6.33	8.40	8.05	7.90	7.86	7.38	7.65	0.67
Eu	2.90	3.46	3.64	3.83	3.42	3.71	3.49	0.30
Gd	6.86	9.55	9.41	8.06	8.79	9.93	8.77	1.04
Tb	1.41	1.61	1.56	1.54	1.30	1.60	1.50	0.11
Dy	9.94	11.0	10.4	10.6	8.28	11.4	10.3	1.00
Ho	2.23	2.54	2.18	2.23	1.66	2.22	2.18	0.26
Er	4.84	6.55	6.29	5.72	4.64	5.90	5.66	0.70
Tm	0.81	0.94	0.73	0.83	0.77	0.92	0.83	0.07
Yb	6.17	5.96	6.10	5.36	5.37	6.28	5.87	0.37
Lu	0.62	0.81	0.69	0.81	0.73	0.71	0.73	0.07
Hf	0.26	0.18	0.20	0.10	0.49	0.33	0.26	0.13
Pb	1.68	1.79	1.71	1.47	1.28	1.72	1.61	0.18
Th	0.48	0.71	0.67	0.72	0.87	1.20	0.78	0.22
U	0.66	1.11	0.80	0.81	0.78	1.82	1.00	0.39

Table S3. (continued)

	plagioclase												
Rim	pl-1	pl-2	pl-3	pl-4	pl-5	pl-6	pl-7	pl-11	pl-12	pl-13	Core pl-14	ave	1σ
V	—	—	—	—	—	—	—	—	—	—	—	—	—
Co	—	—	—	0.60	—	—	—	—	—	1.88	1.88	1.45	0.60
Ni	5.09	9.46	7.96	12.5	6.48	6.30	8.50	12.0	8.78	9.63	7.22	8.54	2.19
Rb	—	—	—	—	—	—	—	—	—	—	—	—	—
Sr	51.7	65.7	76.2	48.3	25.2	34.6	35.7	22.5	25.4	21.8	22.3	39.0	18.1
Y	—	—	—	—	—	—	—	—	0.31	—	—	0.31	—
Zr	—	—	—	—	—	—	—	0.61	5.42	11.0	29.5	11.6	11.0
Nb	—	—	—	—	—	—	—	—	—	—	0.19	0.19	—
Cs	—	—	—	—	—	—	—	—	—	—	—	—	—
Ba	0.98	0.74	0.88	0.69	0.38	0.65	0.51	0.89	0.85	0.52	0.94	0.73	0.19
La	0.03	0.06	0.08	0.08	0.06	0.23	—	0.04	—	—	0.06	0.08	0.06
Ce	0.39	—	0.40	0.05	0.05	0.03	0.05	0.04	0.04	—	0.03	0.12	0.15
Pr	—	—	—	—	0.03	—	—	—	—	—	—	0.03	—
Nd	—	—	—	—	—	—	—	—	—	—	—	—	—
Sm	—	—	—	—	—	—	—	—	—	0.07	—	0.07	—
Eu	—	—	—	—	—	—	—	—	—	—	—	—	—
Gd	—	—	—	—	—	—	—	—	—	0.15	—	0.15	—
Tb	—	—	—	—	—	—	—	—	—	—	—	—	—
Dy	—	—	—	0.04	—	—	—	—	—	—	—	0.04	—
Ho	—	—	—	—	—	—	—	—	0.02	0.03	—	0.03	0.01
Er	—	—	—	—	—	—	0.03	0.03	0.03	0.03	—	0.03	0.00
Tm	—	—	—	—	—	—	—	—	—	—	0.02	0.02	—
Yb	—	—	—	—	—	—	—	—	—	—	—	—	—
Lu	—	—	—	—	—	—	—	—	—	0.03	—	0.03	—
Hf	—	—	—	—	—	—	—	—	0.31	0.28	0.86	0.48	0.27
Pb	0.22	0.20	0.17	0.21	—	0.18	—	—	—	0.29	0.18	0.21	0.04
Th	—	—	0.03	0.04	—	—	—	—	0.01	—	0.01	0.02	0.01
U	—	0.01	—	—	—	—	—	—	—	—	0.01	0.01	—

Table S3. (continued)

	phengite						
	mus-1-1	mus-1-2	mus-2-1	mus-2-2	ave	$1\sigma$	Determination limit
V	251	239	322	294	277	33.3	6.11
Co	29.1	25.3	32.9	28.6	29.0	2.71	0.59
Ni	92.0	77.0	129	114	103	19.9	2.69
Rb	147	128	165	151	148	13.4	0.75
Sr	13.6	12.4	15.8	26.2	17.0	5.47	0.38
Y	—	—	—	—	—	—	0.19
Zr	—	—	0.23	—	0.23	—	0.20
Nb	0.16	—	1.27	2.30	1.24	0.88	0.13
Cs	4.39	4.17	5.00	5.39	4.74	0.48	0.23
Ba	164	165	224	216	192	27.9	0.07
La	0.07	0.10	0.11	0.11	0.10	0.02	0.03
Ce	0.15	—	0.03	0.03	0.07	0.06	0.02
Pr	0.01	0.02	—	—	0.02	—	0.01
Nd	—	—	—	—	—	—	0.07
Sm	—	—	—	—	—	—	0.05
Eu	—	—	—	0.02	0.02	—	0.02
Gd	—	0.08	—	—	0.08	—	0.07
Tb	—	—	—	—	—	—	0.02
Dy	—	—	—	—	—	—	0.04
Ho	—	—	—	—	—	—	0.02
Er	—	—	—	—	—	—	0.03
Tm	—	—	—	—	—	—	0.01
Yb	—	—	—	—	—	—	0.04
Lu	—	—	—	—	—	—	0.01
Hf	—	—	0.05	—	0.05	0.00	0.04
Pb	0.41	0.18	0.17	0.32	0.27	0.10	0.13
Th	—	—	—	—	—	—	0.01
U	—	—	—	—	—	—	0.01

*Table S4. Trace element mineral compositions, mineral/fluid and mineral/mineral partition coefficients and estimated fluid compositions. Concentrations are in ppm*

	Mineral composition				D (mineral/fluid)		D (epi/zoi)	Fluid composition	
	phengite ( <i>n</i> = 4)		epidote ( <i>n</i> = 6)		phengite	zoisite	epi/zoi	estimated from	
	average	1 $\sigma$	average	1 $\sigma$	(Zack01)	(Fein07)	(Chen12)	phengite	epidote
K*	75620	2086	—	—	4.8			15754	
V	277	33.3	185	10.8					
Co	29.0	2.71	3.11	1.89					
Ni	103	19.9	12.4	9.89					
Rb	148	13.4	1.00	0.12	7.8			19	
Sr	17.0	5.47	799	34.1		1842	0.36		1.2
Y	—	—	54.2	4.88					
Zr	0.23	—	9.79	12.8					
Nb	1.24	0.88	11.1	9.88					
Cs	4.74	0.48	—	—	1.0			4.7	
Ba	192	27.9	1.09	0.53	3.5			55	
La	0.10	0.02	13.5	2.17		0.19	4.0		18
Ce	0.07	0.06	37.6	5.69		0.23	4.1		40
Pr	0.02	—	5.33	0.69					
Nd	—	—	25.8	3.96		0.33	4.1		19
Sm	—	—	7.65	0.67		0.63	3.8		3.2
Eu	0.02	—	3.49	0.30		0.93	4.2		0.89
Gd	0.08	—	8.77	1.04					
Tb	—	—	1.50	0.11					
Dy	—	—	10.3	1.00					
Ho	—	—	2.18	0.26		0.34	5.7		1.1
Er	—	—	5.66	0.70					
Tm	—	—	0.83	0.07		0.76	3.8		0.29
Yb	—	—	5.87	0.37		0.85	4.2		1.6
Lu	—	—	0.73	0.07		0.35	4.3		0.48
Hf	0.05	0.00	0.26	0.13					
Pb	0.27	0.10	1.61	0.18		0.49	0.52		6.3
Th	—	—	0.78	0.22					
U	—	—	1.00	0.39					

\*Measured by EPMA, other elements are measured by LA-ICP-MS.

Zack01: Zack et al. (2001); Fein07: extrapolated to 600°C from the data in Feineman et al. (2007); Chen12: Chen et al. (2012).